

<https://helda.helsinki.fi>

Epicardial transplantation of autologous atrial appendage
micrografts : evaluation of safety and feasibility in pigs after
coronary artery occlusion

Nummi, Annu

2022-12-31

Nummi , A , Pätilä , T , Mulari , S , Lampinen , M , Nieminen , T , Mäyränpää , M , Vento , A ,
Harjula , A & Kankuri , E 2022 , ' Epicardial transplantation of autologous atrial appendage
micrografts : evaluation of safety and feasibility in pigs after coronary artery occlusion ' ,
Scandinavian Cardiovascular Journal , vol. 56 , no. 1 , pp. 352-360 . <https://doi.org/10.1080/14017431.2022.2111462>

<http://hdl.handle.net/10138/347764>

<https://doi.org/10.1080/14017431.2022.2111462>

cc_by_nc

publishedVersion

Downloaded from Helda, University of Helsinki institutional repository.

This is an electronic reprint of the original article.

This reprint may differ from the original in pagination and typographic detail.

Please cite the original version.



Epicardial transplantation of autologous atrial appendage micrografts: evaluation of safety and feasibility in pigs after coronary artery occlusion

Annu Nummi, Tommi Pätilä, Severi Mulari, Milla Lampinen, Tuomo Nieminen, Mikko I. Mäyränpää, Antti Vento, Ari Harjula & Esko Kankuri

To cite this article: Annu Nummi, Tommi Pätilä, Severi Mulari, Milla Lampinen, Tuomo Nieminen, Mikko I. Mäyränpää, Antti Vento, Ari Harjula & Esko Kankuri (2022) Epicardial transplantation of autologous atrial appendage micrografts: evaluation of safety and feasibility in pigs after coronary artery occlusion, *Scandinavian Cardiovascular Journal*, 56:1, 352-360, DOI: [10.1080/14017431.2022.2111462](https://doi.org/10.1080/14017431.2022.2111462)

To link to this article: <https://doi.org/10.1080/14017431.2022.2111462>



© 2022 The Author(s). Published by Informa UK Limited, trading as Taylor & Francis Group



[View supplementary material](#)



Published online: 24 Aug 2022.



[Submit your article to this journal](#)



Article views: 162



[View related articles](#)




[View Crossmark data](#)

RESEARCH ARTICLE

 OPEN ACCESS 

Epicardial transplantation of autologous atrial appendage micrografts: evaluation of safety and feasibility in pigs after coronary artery occlusion

Annu Nummi^a, Tommi Pätilä^b, Severi Mulari^a, Milla Lampinen^c, Tuomo Nieminen^{a,d}, Mikko I. Mäyränpää^e , Antti Vento^a, Ari Harjula^a and Esko Kankuri^c

^aHeart and Lung Center, University of Helsinki and Helsinki University Hospital, Helsinki, Finland; ^bPediatric Cardiac Surgery, Children's Hospital, University of Helsinki and Helsinki University Hospital, Helsinki, Finland; ^cDepartment of Pharmacology, Faculty of Medicine, University of Helsinki, Helsinki, Finland; ^dPäijät-Häme Joint Authority for Health and Wellbeing, Lahti, Finland; ^eDepartment of Pathology, University of Helsinki and Helsinki University Hospital, Helsinki, Finland

ABSTRACT

Objectives. Several approaches devised for clinical utilization of cell-based therapies for heart failure often suffer from complex and lengthy preparation stages. Epicardial delivery of autologous atrial appendage micrografts (AAMs) with a clinically used extracellular matrix (ECM) patch provides a straightforward therapy alternative. We evaluated the operative feasibility and the effect of micrografts on the patch-induced epicardial foreign body inflammatory response in a porcine model of myocardial infarction. **Design.** Right atrial appendages were harvested and mechanically processed into AAMs. The left anterior descending coronary artery was ligated to generate acute infarction. Patches of ECM matrix with or without AAMs were transplanted epicardially onto the infarcted area. Four pigs received the ECM and four received the AAMs patch. Cardiac function was studied by echocardiography both preoperatively and at 3-week follow-up. The primary outcome measures were safety and feasibility of the therapy administration, and the secondary outcome was the inflammatory response to ECM. **Results.** Neither AAMs nor ECM patch-related complications were detected during the follow-up time. AAMs patch preparation was feasible according to time and safety. Inflammation was greatly reduced in AAMs when compared with ECM patches as measured by the amount of infiltrated inflammatory cells and area of inflammation. Immunohistochemistry demonstrated an increased CD3⁺ cell density in the AAMs patch infiltrate. **Conclusions.** Epicardial AAMs transplantation demonstrated safety and clinical feasibility. The use of micrografts significantly inhibited ECM-induced foreign body inflammatory reactivity. Transplantation of AAMs shows good clinical applicability as adjuvant therapy to cardiac surgery and can suppress acute inflammatory reactivity.

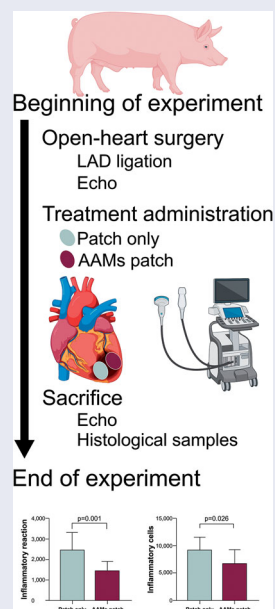
ARTICLE HISTORY



Received 25 May 2022
Revised 4 July 2022
Accepted 5 August 2022


KEYWORDS

Autologous atrial appendage micrografts; atrial appendage stem cells; myocardial infarction; epicardial transplantation; cell therapy

GRAPHICAL ABSTRACT



CONTACT Esko Kankuri  esko.kankuri@helsinki.fi  Department of Pharmacology, Faculty of Medicine, University of Helsinki, PO Box 63 (Haartmaninkatu 8), Helsinki 00014, Finland

 Supplemental data for this article can be accessed online at <https://doi.org/10.1080/14017431.2022.2111462>.

© 2022 The Author(s). Published by Informa UK Limited, trading as Taylor & Francis Group
This is an Open Access article distributed under the terms of the Creative Commons Attribution-NonCommercial License (<http://creativecommons.org/licenses/by-nc/4.0/>), which permits unrestricted non-commercial use, distribution, and reproduction in any medium, provided the original work is properly cited.

Introduction

Myocardial infarction (MI) is a major cause of death worldwide [1]. It bears a poor prognosis particularly when accompanied with ischemic heart failure. Revascularization and medical therapy are critical for severe ischemic heart failure, but the recovery of the irreversibly damaged infarction area is poor or nonexistent. Cell therapy has been proposed as an additional strategy to the current treatment modalities for heart failure: one with potential to restore or even regenerate structure and function of the infarcted area. Several studies have suggested benefit from cell therapies, but therapy preparation suffers from complex and lengthy protocols, and the treatment requires additional interventions. Cell therapies exert their benefit largely through secretion of soluble paracrine factors [2,3]. These protective factors activate pathways in the target tissue that result in the repair and remodeling of infarcted myocardium [4,5]. When administered together with revascularization, cell therapy holds potential to reduce mortality and rehospitalization caused by heart failure during long-term follow-up, improve global left ventricular ejection fraction (LVEF), New York Heart Association (NYHA)—functional class and quality of life as well as to lower poor prognosis-associated high NT-proBNP levels [6]. In our earlier studies the use of injected bone marrow mononuclear cells during coronary artery bypass (CABG) surgery showed significant reduction of MI scar [7,8], which is a major prognostic factor for survival in ischemic heart failure [9,10].

Atrial appendage offers a good tissue-matched reservoir for various cardiac cell types which contribute to paracrine signaling [11–13]. Interestingly, especially the noncardiomyocyte pool has been identified as the dynamically proliferating one and active in the secretion of soluble mediators [14], being thus able to contribute to the mechanically disaggregated atrial appendage's effect on the failing myocardium. The use of autologous cells can minimize rejection and thus ensure better cell engraftment. The extracellular matrix (ECM) and the microtissue architecture of the micrografts can support cellular adherence and survival of transplanted cells [15]. Moreover, the mixture of different myocardial cell types can enable better tissue-mimicking interplay in the micrografts and improve their therapeutic effect via enhanced survival and improved paracrine signaling [16,17].

The effect of any cell therapy is critically dependent on the delivery method [18]. Animal models have proven the epicardial delivery route to be beneficial in securing generous cell engraftment when compared with various types of cell delivery routes by intramyocardial injection or coronary infusion [19,20]. In principle, the technique of delivering progenitor cells epicardially causes minimal harm to the functional myocardium, less arrhythmogenicity [21], and ensures sufficient number of cells to remain at the transplant area [18].

We have reported encouraging results on the transplantation of epicardial atrial appendage micrografts (AAMs) in ischemic heart failure in rodents [22] and from a clinical safety and feasibility trial in patients during CABG surgery

[23,24]. The specific aim of AAMs therapy is to establish a cost-efficient, safe, and clinically feasible micrograft transplant, which would provide functional and structural improvement, activate cardioprotective signaling, reduce infarct scar volume and beneficially modify the myocardium's elasticity. Epicardial transplantation allows the therapy to be well targeted to the damaged area. Based on the current understanding [22], the mode of action is based on paracrine signals, e.g. natriuretic peptides, from the micrografts that activate cardioprotective, angiogenic, and proliferative responses in the damaged myocardium.

This study was established to test the critical technical questions regarding the procedure and ensure the general safety. Specific focus was on the technical details of preparing the transplant (including sterility and time schedule/delay for preparing the transplant during open heart surgery). Additionally, we evaluated the effect of the micrografts on the foreign body reaction and inflammation caused by a pericardial patch ECM sheet in this pig model.

Materials and methods

All procedures on laboratory animals and animal care were approved by the Division of Health and Social Services, Legality and Licensing of the Regional State Administrative Agency for Southern Finland (ESAVI/1482/04.10.07/2015). The study protocol was approved by the Surgical Ethics Committee of the Hospital District of Helsinki and Uusimaa (number 180/13/03/02/13).

The study included eight pigs. Four animals received an ECM patch and four animals an ECM patch with AAMs. The procedure and follow-up were done similarly to all animals.

A standard anterior sternotomy was performed under anesthesia. Before any cardiac interventions, echocardiography (echo) was carried out to assess baseline cardiac function. Then the right atrial appendage (RAA) was ligated using a purse string suture. The RAA was removed from all animals in both groups. The standardized size of the RAA tissue used for AAMs patch was 10 mm × 5 mm. For the animals in the AAMs patch group, the harvested RAA was processed mechanically on-site in the operating room using a tissue homogenizer (Rigenera-system, HBW s.r.l., Turin, Italy) [25]. This system utilizes a sterile, single-use tissue mechanical homogenizer surface to generate the micrografts and yields ~ 5–10 millions of viable cells per gram of RAA tissue [25]. The isolated AAMs were applied in standard cardioplegia suspension, and to seal the micrografts and the suspension to the patch fibrin sealant (Tisseel™, Baxter Healthcare Corp. Westlake Village, CA, USA) was added into the suspension. We used an ECM sheet (Cormatrix® ECMTM Technology, Cormatrix Cardiovascular Inc., Atlanta, GA, USA) as the patch material. The AAMs suspension was placed onto the sheet and the patch was ready to be placed with the AAMs facing the epimyocardium.

MI was introduced by ligating the left anterior descending coronary artery (LAD) with a nonabsorbable suture (Figure 1). Optimal location for ligation was chosen in the

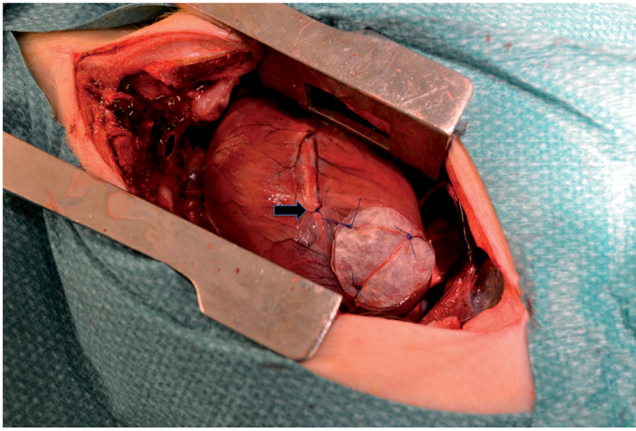


Figure 1. Completed patch at the area of infarct. Completed autologous atrial appendage micrograft (AAMs) patch secured to myocardium with three sutures and ligation of left descending coronary artery causing heart infarct and failure (marked with black arrow).

B-part of the LAD so that the biggest diagonal artery remained untouched and open to secure adequate blood flow to the anterior wall of the left ventricle (LV). This was to make sure that the infarction was large enough to cause observable infarction but the risk for fatal ventricular arrhythmias was controlled. The acute infarction was verified with reduced motion of the inferior wall, accelerated heart rhythm, and local changes in myocardial color.

Approximately 2 h after producing the infarct and careful follow-up of arrhythmias, the Cormatrix[®] with the micrograft suspension was secured to the myocardial surface by three to four simple knots using nonabsorbable suture.

Echo was performed by a single cardiologist. This was carried out on an open heart to achieve adequate vision. Echo was performed twice for each animal under anesthesia; in the beginning of the first operation, prior to the atrial appendectomy and infarction, and at 3-week follow-up when the animals were first put under anesthesia and later euthanized. Echo was done to measure the dimensions of the anterior wall of the LV, to determine the changes in LVEF, and to observe any changes in the cardiac function.

After the operation animals received painkillers (buprenorphine 0.3 mg \times 2–3 and carprofen 50 mg \times 1–2) for 3 days. At the 3 weeks' time point each animal was euthanized and samples from the infarction area with the patch were taken for histological analysis.

Hematoxylin–eosin (HE) staining and immunohistochemistry for CD45, CD3, and CD20 were performed. HE-stained sections were scanned at the digital microscopy and molecular pathology unit [Institute for Molecular Medicine Finland (FIMM), Helsinki, Finland]. Digital images were analyzed using Panoramic Viewer (3DHISTECH Ltd., Budapest, Hungary) and MIPAR[™] image analysis software (Worthington, OH, USA) was used for cell counting. Distance from the Cormatrix[®] inner surface to the epicardium was measured at 10 points from the distant corners of the patch in both groups. At the same distances, squared image samples of 1 mm² were taken and MIPAR[™] was used to calculate number of nuclei and their relative distances in both groups.

The primary antibodies were rabbit anti-CD3 IgG (SP7 monoclonal, Spring Bioscience M3072, Abcam, Cambridge, UK), rabbit anti-CD20 IgG (polyclonal, Thermo Fisher Scientific Labvision RB9013P, Waltham, MA, USA), rabbit anti-CD45 IgG (clone #145 monoclonal recombinant, Sino Biological 100342-R145, Beijing, China). All antibodies were diluted using the antibody diluent (BiositeHisto, Nordic Biosite, Tampere, Finland, cat. no BCB-QUG2XK). Secondary antibody was an HRP-polymer anti-rabbit antibody (BiositeHisto Nordic Biosite cat. no KDB-Z47C3W). Immunoreactivity of antibodies was controlled in sections of porcine kidney, spleen, and liver using human tonsilla as positive control.

Immunohistochemistry was performed at BioSiteHisto Ltd. (Tampere, Finland) using the LabVision Autostainer 480 (Thermo Fisher Scientific) and heat-induced epitope retrieval for 20 min at 98 °C, followed by wash (TBS-TWEEN pH8,4), incubation with primary antibody (30 min, RT), wash, detection polymer incubation (30 min, RT), endogenous peroxidase blocking (10 min, H₂O₂), wash \times 2, DAB (High Contrast DAB, BiositeHisto Nordic Biosite cat. no BCB-R7IKBJ, 10 min, RT), wash, 0,5% CuSO₄-enhancement (10 min), wash, 1:10 Mayer's hemalum solution (Merck KGaA, Darmstadt, Germany, 2 min), bluing with running tap water (7 min), and finally followed by dehydration-clearing. Mounting of coverslips was carried out with xylene-based mounting medium.

Slides were digitalized as WSI in Mirax format with 3DHistech Panoramic MIDI scanner (Budapest, Hungary) at a pixel size of 0.23 μ m \times 0.23 μ m. The scanner utilizes a brightfield microscope setup with an HV_F22CL camera (Hitachi Kokusai Electric America Ltd., Southwick, MA, USA) equipped with a plan-apo 20x objective. For immunostaining analysis, serial non-overlapping images covering the Cormatrix area from every sample were captured with the Panoramic Viewer software (3DHISTECH Ltd.). Image area was then standardized as mm². The analysis of the captured images was carried out using the Fiji ImageJ software [26]. The image analysis macros are available upon request from the corresponding author. Briefly, for each image, after background subtraction, the color deconvolution algorithm to hematoxylin (H) and diaminobenzidine (DAB) channels was utilized. The DAB channel image was thresholded to the stain using the automated default method based on the IsoData algorithm, and the stain intensity was measured. For nuclear counting, hematoxylin-positive nuclei (representing the total amount of nuclei in the image) were counted from the H-channel using the particle-counting algorithm and compared with the thresholded positively immune-stained nuclei counted from the DAB channel. The results of the densitometric image analysis of the serial images for each sample were first averaged, and these single values were then used for the further combined analysis of results. The image analysis macros are available from the authors by request.

The primary outcome measures were safety in terms of hemodynamic adverse effects (ventricular arrhythmias and death) and feasibility of the therapy administration in a

clinical setting. Feasibility was evaluated by the success in completing the delivery of the cell sheet to the infarction area in myocardium and in success in closing the right RAA without any additional suturing. Additional outcome measures were changes in LV wall thickness and in LVEF measured by echo, any problems related to recovery such as infection, lack of normal growth, eating, or exercise and the inflammatory response to ECM.

The groups were compared, and the analyses were performed with SPSS software version 16.0 (Chicago, IL, USA). Two-tailed *t*-test for independent samples was used to compare the groups. Differences were considered significant at $p < .05$. Unless otherwise specified, data in the manuscript are presented as mean \pm SD.

Results

Ten pigs were operated in total. Two pigs died at the table due to ventricular fibrillation after the LAD ligation. Eight surviving pigs underwent the entire study protocol of three weeks. All of them recovered well from the operation, without observable changes in normal physical activity or growth. One animal in the control group had a local abscess beneath the sternal wound while reopening the sternum at the three weeks' time point. Abscess was located below the xiphoid process and was not in contact with the heart or the transplant. There was no further evidence of mediastinitis or sternal infection. This animal was physically in good health without any disturbances in appetite or growth. Other animals showed no signs of wound or other infections.

Feasibility

All eight infarct survivors received the patch successfully. During the observation time of 2 h after the ligation, the patch was ready to be placed in all cases. There was no bleeding in appendages and no additional patching or suturing was needed. The chosen minimum size for the removable appendage tissue was 5 mm \times 10 mm, and the weights ranged 610–830 mg.

Echocardiography

For all pigs, the echo LVEFs evaluated at baseline prior to surgery were normal (LVEF was 70% in all animals). There were no anatomical abnormalities or congenital deficiencies. Each animal's postoperative echo showed hypokinetic area at 3 weeks after surgery, but there were no differences in follow-up LVEFs between the groups (AAMs patch group EF 63.3% \pm 9.4%, range 50–70%; ECM patch group EF 62.5 \pm 4.3%, range 60–70%, $p = .915$).

The mean LV wall thickness (measured at the infarction area) showed no differences between the groups (at baseline AAMs patch group 6.9 mm \pm 0.6 mm, range 5.6–7.3 mm; ECM patch group 6.7 mm \pm 0.7 mm, range 5.7–7.4 mm, $p = .731$; and at follow-up AAMs patch group 7.0 mm \pm 1.8 mm, range 4.6–8.9 mm; ECM patch group

6.8 mm \pm 0.4 mm, range 6.4–7.4 mm, $p = .881$). Thickening of the LV wall during the follow-up was similar between the groups (AAMs patch group 0.3 mm \pm 1.7 mm, range –2.1 mm to 1.7 mm; ECM patch group 0.1 mm \pm 0.6 mm, range –0.85 mm to 0.7 mm, $p = .889$). One animal from the AAMs patch group had severe bleeding during re-sternotomy and the possibility to provide a comparable echo was lost.

Histology

HE-staining showed infiltration of inflammatory cells and foreign body reaction in all animals. This reaction was significantly less in hearts treated with AAMs, when compared with the ECM hearts (Figure 2). The average distance between the Cormatrix[®] and epicardium, representing the thickness of the inflammatory infiltrate, was significantly shorter in the AAMs patch group (AAMs patch group 1463 \pm 441 μ m, range 659–2523 μ m; ECM patch group 2457 \pm 865 μ m, range 1599–4729 μ m, $p = .001$) and the number of inflammatory cell nuclei was significantly less in the AAMs patch group (AAMs patch group 6682/mm² \pm 2475/mm², range 3046–11609/mm²; ECM patch group 8736/mm² \pm 2798/mm², range 5137–13506/mm², $p = .026$, Figure 2). In the ECM patch group, nuclei were clustered, whereas in the AAMs patch group, a more diffuse pattern of the nuclei was observed (Figure 2). In both groups, similarly, the inflammation was evident by migration of giant cell macrophages, neutrophils, eosinophils, and lymphocytes as characterized by HE-staining. Also, there were plenty of capillary vessels along the foreign body reaction without difference between the groups. The inflammation area in all hearts was limited to the area of cell graft or control graft transplant and the endocardial area showed no inflammation. The fibrotic changes due to the infarct were relatively small and mainly seen at the endocardial part of the LV wall. The size of the infarction was variable in both groups and all animals. Only a few samples (from three animals) showed larger infarcts with granulation tissue and small calcification and necrotic areas with no difference between the groups. By the histological evaluation used for this study, no transplanted micrografts or cells were observed.

The results from immunohistochemistry analysis of the inflammatory infiltrates' cell densities are presented in Table 1. CD3⁺ cell density, representing the T-lymphocyte density, was greater in AAMs patch group (AAMs patch group 4834/mm² \pm 1271/mm², range 3028–7131/mm²; ECM patch group 3364/mm² \pm 667/mm², range 2336–5346/mm², $p < .001$, Figure 3). Moreover, mean intensity was stronger in the AAM patch group in CD3 staining (AAMs patch group 126/mm² \pm 12/mm², range 107–146/mm²; ECM patch group 114/mm² \pm 9.8/mm², range 87–124/mm², $p = .007$). Density of CD45⁺ cells, representing total lymphocyte density, was not significantly different between groups (AAMs patch group 6376/mm² \pm 1990/mm², range 4009–14748/mm²; ECM patch group 5467/mm² \pm 1579/mm², range 3159–9925/mm², $p = .078$, Figure 4). Mean intensity in CD45 staining did not reach statistical difference between groups. There

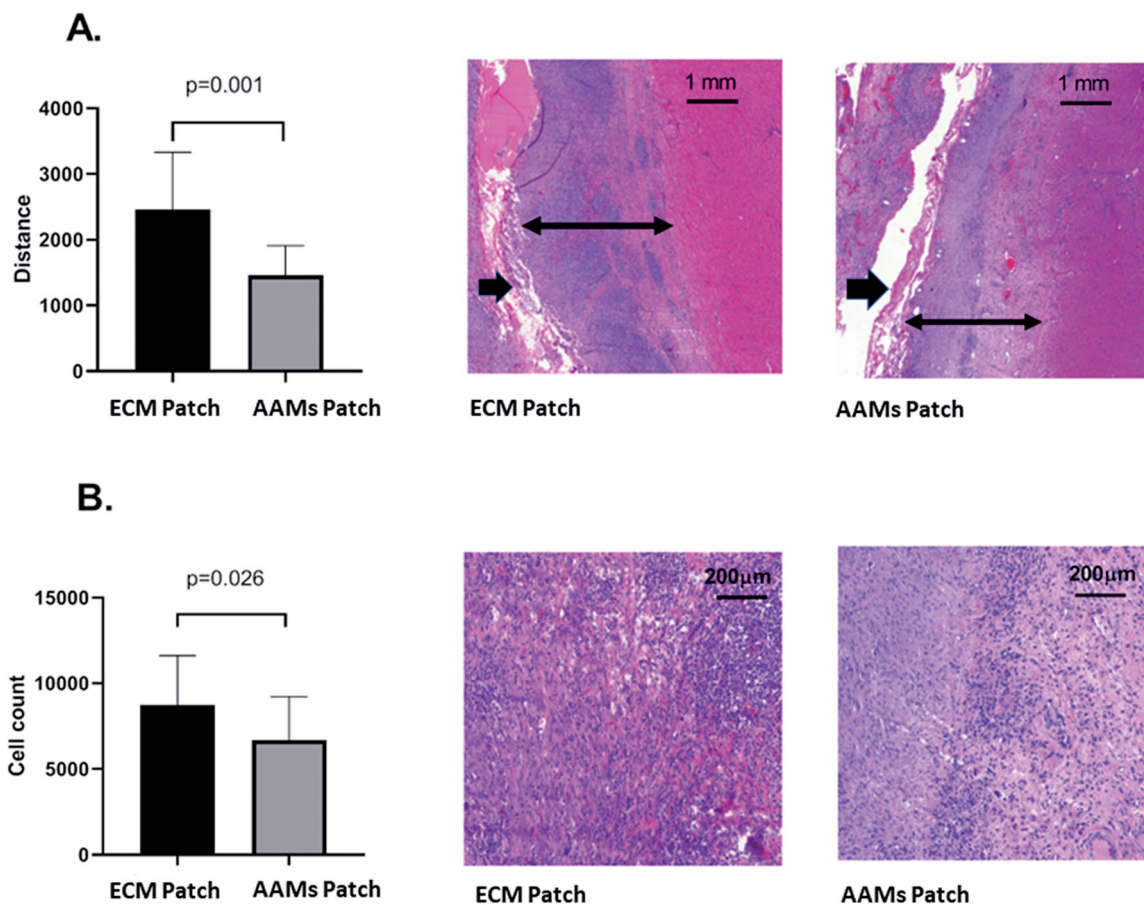


Figure 2. Comparison of inflammatory reaction by hematoxylin–eosin staining. Hematoxylin–eosin staining from the area of the ECM patch (marked with single arrow) and myocardium. (A) Figure shows average distance from the ECM patch to epicardium (average of 10 measurements). A representative distance measurement shown with double red arrow. In autologous atrial appendix micrografts (AAMs)-containing samples this distance was significantly less than in samples without AAMs. Scalebar 1 mm. (B) Figure showing cell count from the foreign body reaction caused by the patch. Inflammation was more cell dense in control samples whereas the AAMs group showed more diffusely scattered nuclei at the supra-epicardial area. The cell nuclei per 1 mm² count was performed twice from each sample. Scalebar 200 μ m.

Table 1. Results and comparison of nuclei from immunohistochemistry staining.

	Cell	Cormatrix	<i>p</i> Value
CD3			
No. of positive stained cells/mm ²	4834 \pm 1271 (3028–7131)	3364 \pm 667 (2336–5346)	<.001
Mean intensity	126 \pm 12 (107–146)	114 \pm 9.8 (87–124)	.007
Stained area out of total area (%)	26 \pm 6.0 (15–34)	21 \pm 7.0 (7.9–32)	.107
CD45			
No. of positive stained cells/mm ²	6376 \pm 1990 (4009–14748)	5467 \pm 1579 (3159–9925)	.078
Mean intensity	140 \pm 21 (109–192)	129 \pm 13 (110–151)	.100
Stained area out of total area (%)	42 \pm 4.5 (34–50)	42 \pm 7.4 (25–54)	.659
CD20			
No. of positive stained cells/mm ²	700 \pm 277 (346–1069)	682 \pm 389 (238–1552)	.703
Mean intensity	137 \pm 9.7 (124–152)	146 \pm 29 (91–198)	.531
Stained area out of total area (%)	17 \pm 5.4 (6.9–24)	15 \pm 7.9 (3.9–33)	.433

CD3 represents T-lymphocyte population in tissue samples, CD45 represents overall lymphocyte population in tissue samples, and CD20 represents B-lymphocyte population in tissue samples.

were also no differences in the CD20⁺ cell densities between groups (Figure 5).

Discussion

The specific aim of this study was to evaluate the safety and feasibility of epicardial delivery of AAMs in pigs after MI. We found that epicardial transplantation was both feasible and safe using this large animal model.

Ventricular fibrillation occurred in two out of ten pigs (20%). These arrhythmias occurred immediately after ligation of the LAD and caused the death of both animals. The reported mortality rates in porcine models of infarction are usually high, 33% [27] due to the susceptibility of pigs developing fatal arrhythmias after coronary occlusion. The infarction in our study was therefore not too large to cause death but adequate to cause local changes and clearly observable acute ischemia.

All eight pigs receiving therapy recovered well and survived the 3 week follow-up. Even though the hypokinetic area in the inferior and anterior wall of LV was seen in echo, the infarction changes seen at histological evaluation were not constantly observable in every section. In one

histological cross-section, the left descending artery was reopened for blood flow due to the collateral connections. The natural capacity of these adolescent pigs to recover was most likely the reason for only little permanent damage caused by the infarction [28].

In all samples, an active foreign body reaction was detected with leukocytes including macrophages, eosinophils, and lymphocytes. There was, however, a significant difference in the amount of inflammation among the two groups. The number of inflammatory cell nuclei in the AAMs patch group samples was significantly less as measured by counting the amount of nuclei and the area foreign body reaction when compared with the ECM patch group. The cells and micrografts inside the transplant were clearly protecting against the foreign body reaction. This may be explained by the paracrine effect of transplanted cells. Transplanted cells release protective factors and signals that have been proven to be the main reason for environmental tissue repair and remodeling. These signals (including cytokines, chemokines, growth factors, and extracellular vesicles) activate pathways which consecutively improve blood perfusion, tissue repair, and remodeling and inhibit hypertrophy and fibrosis [29–31]. Extracellular vesicles such as exosomes are one key type of cell signaling and cell-derived communication which occurs between the AAMs and the myocardium. Exosomes have been reported to increase cell proliferation, reduce infarct size and increase EF in animal studies [32,33]. In addition these cardioprotective secreted vesicles have also been reported to inhibit unwanted inflammation [3–5] via, for example, activation of macrophages, cell apoptosis, and increase in metabolism [3,5]. This protective force against inflammation that transplanted cells possess may contribute to the reduced inflammatory reaction when micrografts were used compared with the ECM sheet alone. We found no signs of the transplanted micrografts or cells in histological evaluation. We, however, have demonstrated in our previous study [22] with rodents that the micrograft survival was ~2 months after the transplantation. The survival and fate of the micrografts deserves further study in a relevant animal model.

Cormatrix[®], decellularized porcine small intestine submucosa, is clinically used as a scaffold to support tissue

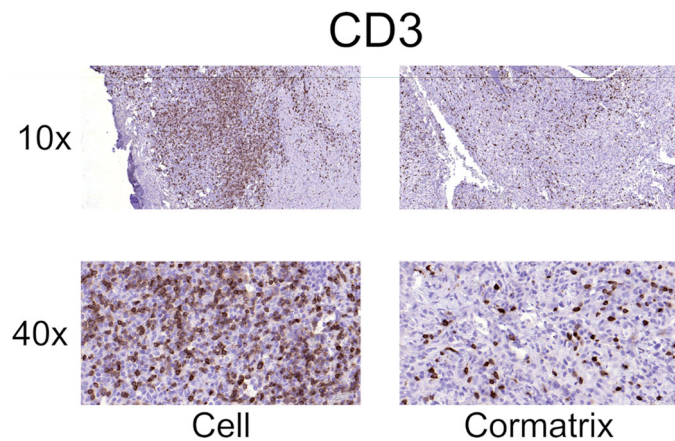


Figure 3. Representative immunohistochemistry images for T-lymphocytes (CD3+) from the AAMs patch group (left panels) and ECM patch group (right panels). Demonstrating figure for T-lymphocyte population (CD3+) in tissue plate staining between the groups.

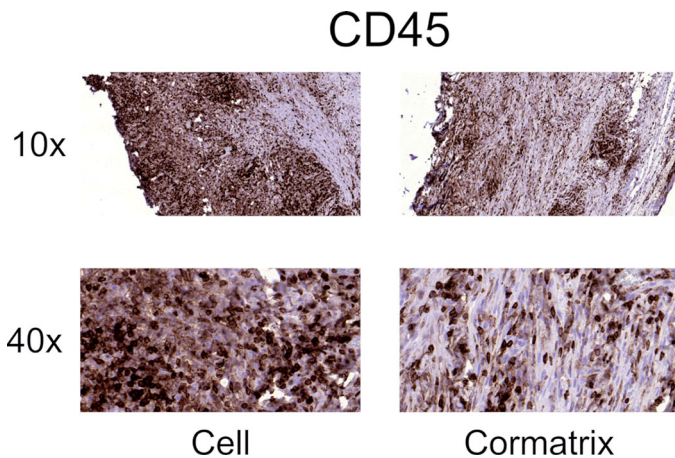


Figure 4. Representative immunohistochemistry images for leukocytes (CD45+) from the AAMs patch group (left panels) and ECM patch group (right panels). Demonstrating figure for overall lymphocyte population (CD45+) in tissue plate staining between the groups.

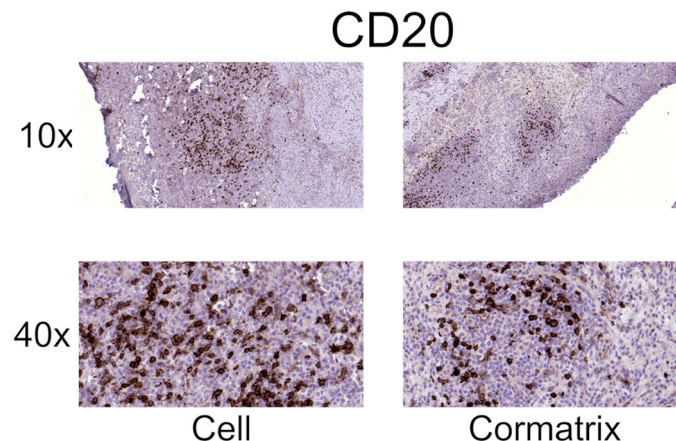


Figure 5. Representative immunohistochemistry images for B-cells (CD20+) from the AAMs patch group (left panels) and ECM patch group (right panels). Demonstrating figure for B-cell population (CD20+) in tissue plate staining between the groups.

regrowth in vascular structures. This ECM is gradually replaced, leaving behind functional tissue. Several studies have shown that Cormatrix[®] elicits inflammatory reactions [34–37] as also clearly seen in our study. Inflammation is histologically seen mainly in eosinophilic infiltrates often with granulation tissue, fibrosis [38], and foreign body giant cell reaction [39]. Therefore, knowing the inflammatory response that Cormatrix[®] causes, especially in porcine, the differences in strength of the foreign body reaction compared with the use of AAMs and ECM matrix alone was the most important finding and the main focus in histologic evaluation. The use of AAMs seemed to inhibit the inflammatory effect of Cormatrix[®] and therefore result in a more satisfying environment.

It has been proven that the use of biological material alone may have a beneficial effect to the infarcted myocardium. This is possible due to the fact that the material placed on myocardium seems to thicken the wall, reduce wall stress, and eventually prevent the negative LV remodeling [40]. This was also seen in our study. There were no differences in LV wall measures or LVEF between the two groups. The infarcted wall was performing equally well whether the micrografts were or were not used with the supportive matrix.

The number of cardiomyocytes in adult heart remains approximately the same during a lifetime [41,42] and the growth in adult mammalian heart occurs in cell size rather than increase in cells. Despite numerous efforts to generate new cardiac muscle cells via stem/progenitor cell technologies, there is no desired outcome. Bin Zhou and colleagues provided evidence that there is no cardiomyocyte producing stem cell population in the adult mammalian heart [43]. Yet there are promising results documented in improvement of LVEF, ventricular remodeling, and reduction of the infarct scar in both preclinical and clinical studies with stem cells [38–45]. With this paradoxical result, further investigations, especially focusing on elucidating the mechanism of action, on cell therapy in heart failure are necessary. The effect and importance of paracrine signaling, different delivery methods, cell sources, and used cell types all need better understanding and more large-scale, randomized trials.

Our results demonstrate that atrial micrografts can modulate and suppress the immune response, as mimicked here by the foreign body response to biomaterial, by shifting the leucocyte balance toward a more CD3+ T-cell-populated one. Through the production of cytokines and chemokines [46,47], the T-helper (Th) cells (especially Th1, Th2, and Th17 cells) modulate the inflammatory response within their microenvironment through secretion of cytokines and chemokines [39]. In this study, our results demonstrate that AAMs treatment alters the cellular enrichment of the foreign body inflammatory infiltrate caused by the ECM. After AAMs treatment, the overall inflammatory reaction is diminished, there are less inflammatory cells and the infiltrated cell population is T-lymphocyte-enriched rather than enriched with B-lymphocytes, neutrophils, or eosinophils. Observed in this study as a secondary endpoint, this

inflammatory reaction modulatory activity of the AAMs requires further targeted investigations.

These results may have important implications for the treatment of acute inflammatory reactions, for example, acute MIs, with AAMs. Our results provide the first insight into the regulation of the inflammatory and immune responses by AAMs. Further investigations should be targeted toward the identification of leukocyte polarization and especially the anti-inflammatory subtype analysis of leukocytes and T-cells after AAMs treatment. Moreover, these experiments should utilize various inductors of inflammation and immune responses.

Conclusions

The Cormatrix ECM sheet causes substantial inflammatory response to adjacent tissues in the porcine, while myocardium stays intact in this response. Additional delivery of AAMs attenuates the inflammatory response, while keeping the regenerative potential as effective, providing a clinically feasible additive for the goal to repair the infarcted myocardium. Transplantation of AAMs with ECM shows good clinical applicability as adjuvant therapy to cardiac surgery and may serve as a potential delivery platform for future cell- or gene-based cardiac therapies.

Acknowledgements

Research nurses Liisa Blubaum, Anna Blubaum, and Mariitta Salmi are gratefully acknowledged and thanked for their professional expertise in the development of the protocol. Technicians Olli Valtanen and Veikko Huusko are thanked for their help and professional contribution in animal laboratory. We gratefully acknowledge BioSiteHisto Ltd. (Tampere, Finland) and MSc Johanna Lappeteläinen for performing the immunohistochemistry experiments. The authors express gratitude and acknowledgement to the AADC Consortium for professional collaboration and academic excellence in the field. We also want to thank Helsinki University Library for funding the Open access.

Author contributions

Conceptualization: AN, TP, ML, TN, AV, AH, and EK; Data curation: SM; Formal analysis: SM and MIM; Funding acquisition: AN, AV, AH, and EK; Investigation: AN, ML, MIM, and EK; Methodology: AN and EK; Project administration: AN, TP, SM, ML, TN, and EK; Resources: AV; Supervision: AV, AH, and EK; Validation: MIM; Writing—original draft: AN and SM; Writing—review and editing: AN, TP, ML, TN, MIM, AV, AH, and EK All authors read and approved the final manuscript.

Disclosure statement

AN and EK are stakeholders in EpiHeart Ltd. developing medical devices for the operating room. Other authors declare no competing interests for this article.

Funding

This work was supported by Ari Harjula, Antti Vento, and Annu Nummi by Finnish Government Block Grants for Clinical Research [grant numbers TYH Y2016SK013, TYH2016211, TYH2015311,

TYH2019266, and Y1016SK017], Esko Kankuri by Finnish Funding Agency for Technology and Innovation [grant number 40033/14], Annu Nummi by Finnish Society of Angiology and Mikko I. Mäyränpää by The Finnish Medical Foundation.

ORCID

Mikko I. Mäyränpää  <http://orcid.org/0000-0002-0877-9640>

Data availability statement

The data that support the findings of this study are available from the corresponding author, Esko Kankuri, upon reasonable request.

References

- [1] GBD 2015 Mortality and Causes of Death Collaborators. Global, regional, and national life expectancy, all-cause mortality, and cause-specific mortality for 249 causes of death, 1980–2015: a systematic analysis for the Global Burden of Disease Study 2015. *Lancet* 2016;388:1459–1544.
- [2] Nguyen PK, Rhee JW, Wu JC. Adult stem cell therapy and heart failure, 2000 to 2016: a systematic review. *JAMA Cardiol.* 2016;1(7):831–841.
- [3] Gnecci M, Zhang Z, Ni A, et al. Paracrine mechanisms in adult stem cell signaling and therapy. *Circ Res.* 2008;103(11):1204–1219.
- [4] Gnecci M, He H, Liang OD, et al. Paracrine action accounts for marked protection of ischemic heart by Akt-modified mesenchymal stem cells. *Nat Med.* 2005;11(4):367–368.
- [5] Stempien-Otero A, Helterline D, Plummer T, et al. Mechanisms of bone marrow-derived cell therapy in ischemic cardiomyopathy with left ventricular assist device bridge to transplant. *J Am Coll Cardiol.* 2015;65(14):1424–1434.
- [6] Fisher SA, Doree C, Mathur A, et al. Meta-analysis of cell therapy trials for patient with heart failure. *Circ Res.* 2015;116(8):1361–1377.
- [7] Pätälä T, Lehtinen M, Vento A, et al. Autologous bone marrow mononuclear cell transplantation in ischemic heart failure: a prospective, controlled, randomized, double-blind study of cell transplantation combined with coronary bypass. *J Heart Lung Transplant.* 2014;33(6):567–574.
- [8] Lehtinen M, Pätälä T, Vento A, Helsinki BMMC Collaboration, et al. Prospective, randomized, double-blinded trial of bone marrow cell transplantation combined with coronary surgery-perioperative safety study. *Interact Cardiovasc Thorac Surg.* 2014;19(6):990–996.
- [9] Wu KC, Zerhouni EA, Judd RM, et al. Prognostic significance of microvascular obstruction by magnetic resonance imaging in patients with acute myocardial infarction. *Circulation.* 1998;97(8):765–772.
- [10] Kelle S, Roes SD, Klein C, et al. Prognostic value of myocardial infarct size and contractile reserve using magnetic resonance imaging. *J Am Coll Cardiol.* 2009;54(19):1770–1777.
- [11] Koninckx R, Daniels A, Windmolders S, et al. The cardiac atrial appendage stem cell: a new and promising candidate for myocardial repair. *Cardiovasc Res.* 2013;97(3):413–423.
- [12] Itzhaki-Alfia A, Leor J, Raanani E, et al. Patient characteristics and cell source determine the number of isolated human cardiac progenitor cells. *Circulation* 2009;120(25):2559–2566.
- [13] Mishra R, Vijayan K, Colletti EJ, et al. Characterization and functionality of cardiac progenitor cells in congenital heart patients. *Circulation* 2011;123(4):364–373.
- [14] Kretzschmar K, Post Y, Bannier-Hélaouët M, et al. Profiling proliferative cells and their progeny in damaged murine hearts. *Proc Natl Acad Sci USA* 2018;115(52):E12245–E12254. 26
- [15] Steinhauser ML, Lee RT. Regeneration of the heart. *EMBO Mol Med.* 2011;3(12):701–712.
- [16] Lampinen M, Vento A, Laurikka J, et al. Rational autologous cell sources for therapy of heart failure—vehicles and targets for gene and RNA therapies. *Curr Gene Ther.* 2016;16(1):21–33.
- [17] Dobaczewski M, Gonzalez-Quesada C, Frangogiannis NG. The extracellular matrix as a modulator of the inflammatory and reparative response following myocardial infarction. *J Mol Cell Cardiol.* 2010;48(3):504–511.
- [18] Fukushima S, Sawa Y, Suzuki K. Choice of cell-delivery route for successful cell transplantation therapy for the heart. *Future Cardiol.* 2013;9(2):215–227.
- [19] Fisher SA, Brunskill SJ, Doree C. Stem cell therapy for chronic ischaemic heart disease and congestive heart failure. *Cochrane Database Syst Rev.* 2014;4:CD007888.
- [20] Wen Y, Meng L, Xie J, et al. Direct autologous bone marrow-derived stem cell transplantation for ischemic heart disease: a Meta-analysis. *Expert Opin Biol Ther.* 2011;11(5):559–567.
- [21] Pätälä T, Miyagawa S, Imanishi Y, et al. Comparison of arrhythmogenicity and proinflammatory activity induced by intramyocardial or epicardial myoblast sheet delivery in a rat model of ischemic heart failure. *PLoS ONE.* 2015;10(4):e0123963.
- [22] Yanbo X, Lampinen M, Takala J, AADC consortium, et al. Epicardial therapy with atrial appendage micrografts salvages myocardium after infarction. *J Heart Lung Transplant.* 2020;39(7):707–718.
- [23] Nummi A, Nieminen T, Pätälä T, AADC consortium, et al. Epicardial delivery of autologous atrial appendage micrografts during coronary artery bypass surgery—safety and feasibility study. *Pilot Feasibility Stud.* 2017;3:74.
- [24] Lampinen M, Nummi A, Nieminen T, AADC Consortium, et al. Intraoperative processing and epicardial transplantation of autologous atrial tissue for cardiac repair. *J Heart Lung Transplant.* 2017;36(9):1020–1022.
- [25] Trovato L, Monti M, Del Fante C, et al. A new medical device rigeneracons allows to obtain viable micro-grafts from mechanical disaggregation of human tissues. *J Cell Physiol.* 2015;230(10):2299–2303.
- [26] Schindeli J, Arganda-Carreras I, Frise E, et al. Fiji: an open-source platform for biological-image analysis. *Nat Methods* 2012;9(7):676–682.
- [27] Kraitchman DL, Bluemke DA, Chin BB, et al. A minimally invasive method for creating coronary stenosis in a swine model for MRI and SPECT imaging. *Invest Radiol.* 2000;35:445–451.
- [28] Pätälä T, Ikonen T, Kankuri E, et al. Spontaneous recovery of myocardial function after ligation of ameroid-stenosed coronary artery. *Scand Cardiovasc J.* 2009;43(6):408–416.
- [29] Tang XL, Rokosh G, Sanganalmath SK, et al. Intracoronary administration of cardiac progenitor cells alleviates left ventricular dysfunction in rats with a 30-day-old infarction. *Circulation* 2010;121(2):293–305.
- [30] Farahmand P, Lai TY, Weisel RD, et al. Skeletal myoblasts preserve remote matrix architecture and global function when implanted early or late after coronary ligation into infarcted or remote myocardium. *Circulation* 2008;118(14_suppl_1):130–137.
- [31] Mathieu M, Bartunek J, El Oumeiri B, et al. Cell therapy with autologous bone marrow mononuclear stem cells is associated with superior cardiac recovery compared with use of nonmodified mesenchymal stem cells in a canine model of chronic myocardial infarction. *J Thorac Cardiovasc Surg.* 2009;138(3):646–653.
- [32] Lai RC, Arslan F, Lee MM, et al. Exosome secreted by MSC reduces myocardial ischemia/reperfusion injury. *Stem Cell Res.* 2010;4(3):214–222.
- [33] Arslan F, Lai RC, Smeets MB, et al. Mesenchymal stem cell-derived exosomes increase ATP levels, decrease oxidative stress and activate PI3K/Akt pathway to enhance myocardial viability and prevent adverse remodeling after myocardial ischemia/reperfusion injury. *Stem Cell Res.* 2013;10(3):301–312.

- [34] Zaidi AH, Nathan M, Emani S, et al. Preliminary experience with porcine intestinal submucosa (CorMatrix) for valve reconstruction in congenital heart disease: histologic evaluation of explanted valves. *J Thorac Cardiovasc Surg.* **2014**;148(5):2216–4, 2225e1.
- [35] Wells WJ. Responsible innovation. *J Thorac Cardiovasc Surg.* **2014**;148(5):2225–2226.
- [36] Rosario-Quinones F, Magid MS, Yau J, et al. Tissue reaction to porcine intestinal submucosa (CorMatrix) implants in pediatric cardiac patients: a single-center experience. *Ann Thorac Surg.* **2015**;99(4):1373–1377.
- [37] Nelson JS, Heider A, Si M-S, et al. Evaluation of explanted cor-matrix intracardiac patches in children with congenital heart disease presented at the fifty-second. *Ann Thorac Surg.* **2016**;102(4):1329–1335.
- [38] Cong XQ, Li Y, Zhao X, et al. Short-term effect of autologous bone marrow stem cells to treat acute myocardial infarction: a Meta-analysis of randomized controlled clinical trials. *J Cardiovasc Transl Res.* **2015**;8(4):221–231.
- [39] Zhu J, Yamane H, Paul WE. Differentiation of effector CD4 T cell populations. *Annu Rev Immunol.* **2010**;28:445–489.
- [40] Radisic M, Christman KL. Materials science and tissue engineering: repairing the heart. *Mayo Clin Proc.* **2013**;88(8):884–898.
- [41] Burridge PW, Thompson S, Millrod MA, et al. A universal system for highly efficient cardiac differentiation of human induced pluripotent stem cells that eliminates interline variability. *PLoS One* **2011**;6(4):e18293.
- [42] Burridge PW, Keller G, Gold JD, et al. Production of de novo cardiomyocytes: human pluripotent stem cell differentiation and direct reprogramming. *Cell Stem Cell* **2012**;10(1):16–28.
- [43] Li Y, He L, Huang X, et al. Genetic lineage tracing of population by dual recombinases. *Circulation* **2018**;138(8):793–805.
- [44] Henry TD, Pepine CJ, Lambert CR, et al. The athena trials: autologous adipose-derived regenerative cells for refractory chronic myocardial ischemia with left ventricular dysfunction. *Catheter Cardiovasc Interv.* **2017**;89(2):169–177.
- [45] Gyöngyösi M, Wojakowski W, Lemarchand P, ACCRUE Investigators, et al. Meta-analysis of cell-based CaRdiac stUdiEs (ACCRUE) in patients with acute myocardial infarction based on individual patient data. *Circ Res.* **2015**;116(8):1346–1360.
- [46] Romagnani S. Lymphokine production by human T cells in disease states. *Annu Rev Immunol.* **1994**;12:227–257.
- [47] Annunziato F, Cosmi L, Romagnani S. Human and murine Th17. *Curr Opin HIV AIDS.* **2010**;5:114–119.